

Synthesis and Characterization of Magnetic Graphene-Oxide

Abstract: In this present work, we report the synthesis of Graphene oxide based magnetic nano-composites with the size of (~13-14 nm) using simple chemical co-precipitation method. The composites were characterized by X-ray diffraction (XRD), Fourier transform infrared spectroscopy (FTIR) and vibrating sample measurement (VSM). It was observed that all the composites are superparamagnetic in nature. The saturation magnetization was observed to increase with the increasing magnetite nanoparticles (MNPs) in the composites. The dielectric properties of the composites were also improved by adding magnetites NPs. These results remark that synthesized nanocomposites have great potential for magnetic, capacitive and microwave absorption applications.

Keywords: Graphen-Oxide, Magnetic Graphene-Oxide, Hysteresis, Dielectric Loss.

Introduction: The graphene is a single or multi-layer 2D hexagonal honeycomb lattice sheet. These sheets are sp^2 hybridized and are separated about 1.4 \AA from each other thus increasing the sheet strength [1]. Due to two-dimensional nature along with associated band structure, graphene and its composites are utilized in various applications such as supercapacitors, electronics, biosensing and photocatalysis[2-4]. Graphene and its derivative form graphene oxide are obtained from graphite [5]. GO consists the polar surfaces with then attached functional groups C=O,C-O and -OH. Due to this polar surfaces , a number of materials like bio-molecules, metals, fluorescent moieties, drug molecules and nanoparticles can be easily attached with GO [1].

Due to their unique chemical, physical, thermal and mechanical properties, magnetite nanoparticles (MNPs) offer a high potential for several applications in the field of environmental remediation, water purification, , magnetic recording media, data storage, ferro-fluids as well as

in various biomedical applications etc [6-8]. On other hand, MNPs has the large surface to volume ratio and therefore posses high surface energies. Then, they tend to aggregate so as to minimize the surface energies for being stable. Moreover, the MNPs have high chemical activity and easily oxidized in air resulting loss in magnetism. This comprise coating and grafting with organic molecules or surfactants, polymers, inorganic layes such as silica, metal, nonmetal etc [9].

Nano-composites of MNPs with GO have drawn a lot of attention due to their extensive applications in various fields such as drug delivery [10], water purification [11], batteries [12], environmental remediation[13],electro-magnetic shielding [14], water purification [15], microwave absorption [16], sensors [17] and bio-medical etc. In the present work, we have fabricated graphene oxide doped magnetite nanocomposites (GOMNCs) with different weight ratios using chemical co-precipitation method. The structural, thermal, electrical and magnetic properties of prepared nanostructures were compared with that of GO and GOMNCs.

2. Experimental:

2.1. Materials: Grapheme oxide , $\text{FeCl}_2 \cdot 4\text{H}_2\text{O}$, anhydrous FeCl_3 , ammonia solution, hydrogen peroxide solution , sulfuric acid, hydrochloric acid and de-ionized water were used for the preparation of composites.

2.2 Preparation of GO- Fe_3O_4 composites

GO was prepared according to literature reports via modified Hummer's method [18]. GOMNCs were prepared through chemical co-precipitation of Fe_3O_4 from a composition of $\text{FeCl}_2 \cdot 4\text{H}_2\text{O}$ and $\text{FeCl}_3 \cdot 6\text{H}_2\text{O}$ in 1:2 molar ratio supplemented with varying weight fractions of GO. The weight fractions of Fe (III) to GO was adjusted into 5:1, 8:1, 15:1 to afford the three samples of GOMNCs. For the preparation of GOMNCs involving Fe (III): GO (I), a suspension of GO (0.1g/dL, 50 mL) in deionized water was subjected to ultrasonic treatment over 45 min with simultaneous feeding of 50 mL a formulation of Fe (III):Fe (II) in 1:0.6 (w/w,50 mL) in deionized water @ 0.1 mL/min at 300K. Chemical co-precipitation of Fe_3O_4 in presence of GO was conducted through addition of ammonia solution (30%,v/v) at 85⁰C till rise in pH level of reaction medium to 10.The contents were allowed for stirring @500 rpm over 180 min thereafter

cooled to 300K and subsequently centrifuged at ~4000 rpm for 15 min. GOMNCs settled at the bottom of centrifuge tube were successively washed with deionized water till removal of chloride ions. GOMNCs were isolated from centrifuge tube through magnetic separation and dried at 400 mmHg/300K. Magnetite nanoparticles were also prepared following identical co precipitation method and served as reference for measurement of spectral and electrical, thermal and magnetic properties of GOMNCs.

2.2 Characterization:

The structure of nanocomposites is being characterized using X-Ray Diffraction (Bruker D8 ADVANCE) with Cu K α irradiation ($\lambda = 1.5406 \text{ \AA}$), and Fourier transform infrared (FT-IR) spectroscopy over the spectral range of 4000–500 cm^{-1} (Perkin Elmer Spectrum Two Version 10.03.06 with KBr pellets) to determine their crystal structure, bonding behavior and functional groups. The composition and morphology are being determined using Scanning Electron Microscopy technique. The optical and magnetic properties are being studied using UV–Visible spectrophotometer and Vibrating Sample Magnetometer (VSM) respectively. Average crystallite size (D) of samples was calculated using Scherrer's formula $D = 0.93\lambda / \beta \cos\theta$, where λ is the X-ray wavelength, β is the full width at half maximum in radian and θ is the angle of diffraction. The room temperature (300K) magnetic properties of synthesized samples were studied using vibrating sample magnetometer (Quantum design PPMs, temp-range upto 2K, magnetic field-9 tesla). Dielectric measurements were performed for the frequency range 100 Hz and 1MHz using Automatic Hioki 3532-50 Hi teater LCR meter.

3. Results and discussion

3.1 Microstructure

The surface morphology of the GOMNCs were found out by using scanning electron microscopy. SEM images fig. 1 show that GOMNCs are spherical in shape with a narrow particle size (~12-14 nm which is calculated by the Debye–Scherrer formula). Particles agglomeration is indicating a good connectivity between the grains all together. It looks like a smoothed sponge-like structure.

The X-ray diffraction pattern of natural graphite powder, GO and GOMNCs were shown in Fig.2. Graphite shows a lattice planes of (002), (101) and (004) at $2\theta = 26.8^\circ$, 44.8° 54.8° respectively with 0.33 nm spacing between the layers [5]. In the XRD pattern GO, peak (002) is shifted to 11.94° , indicating that the interlayer spacing increases to 0.74 nm after oxidization [18-19]. Due to the existence of oxygen functional groups, the interplanar spacing of GO is increased. XRD reveals the formation of MNPs with crystallite size ~ 17.5 nm bearing single-phase cubic spinel and lattice parameter 8.36\AA [20]. Addition of magnetite nanoparticles into GO rendered a series of diffraction peaks at angles 2θ (plane) = 30.30° (220), 35.66° (311), 43.35° (400), 57.3° (511), 63.0° (440). Except the diffraction peaks assigned to magnetite nanoparticles, no other characteristic peaks result from GO can be observed in the XRD pattern of the composites system. It demonstrates the complete reduction of the GO. Moreover, there is no outstanding diffraction peak at $\sim 26^\circ$ as the result of uniform dispersion of GO on the surface of magnetite NPs, indicating exfoliation and preventing another restacking of the graphene sheets to larger extent [21]. The addition of GO has induced a surprising reduction in the crystallite size of magnetite NPs ranging 17.50 to 13-14 nm with retained cubic structure.

3.2 FTIR study

The FTIR spectra of GO and GOMNCs are shown in Fig.3. Upon oxidation of graphite to GO, the observed representative peaks of GO confirm the presence of the oxygen-containing functional moieties in carbon frameworks, which include the bands at $\sim 1040\text{ cm}^{-1}$ (C-O stretching vibration of epoxide), 1420 cm^{-1} (tertiary C-OH groups stretching), and 1720 cm^{-1} (C=O stretching of carbonyl and carboxyl groups located at edges of the GO networks). Moreover, signature of aromatic C=C stretching at $\sim 1576\text{ cm}^{-1}$ indicates the presence of sp^2 hybridized honeycomb lattice [22]. Peak around at 3414 cm^{-1} shows that moisture content in GO. The small signals located at 1965 cm^{-1} may belong to aromatic ring. These bands confirm the formation of GO from the oxidation of graphite powder.

In the FTIR spectrum, there are normally four sets of lattice vibrations, corresponding to lower and higher frequencies. The lattice vibrations involving oxygen and cations at octahedral and tetrahedral positions in the base lattice appear in the high frequency region, namely, ν_1 and ν_2 at $600\text{--}540\text{ cm}^{-1}$ and $400\text{--}460\text{ cm}^{-1}$, respectively. The low frequency bands in the vicinity of 320 cm^{-1} are due to divalent oxygen vibrations. The typical M-O bond corresponds to a major

banding the range of 550 to 553 cm^{-1} (tetrahedral) and a faint peak at 430 cm^{-1} (octahedral lattice vibrations). The peak at 1387 cm^{-1} is due to the asymmetrical stretching vibrations of adsorbed carbonate ions CO_3^{2-} on the lattice.

In the FTIR spectrum of GOMNCs, band ranging 445 cm^{-1} -625 cm^{-1} attributed to vibrational modes of Fe-O confirms the occupancy of ferric ion (Fe^{+3}) at tetrahedral sites. The band at about 453 cm^{-1} corresponds to the presence of Fe-O bond at octahedral sites in the composites due to the magnetite phase [23-24].

3.4. Thermal studies

The TG thermogram of GO also reveals the two step decomposition behavior (Fig. 4 (a)). The first weight loss 8.27 % of GO occurs in the temperature range of 30⁰ C -105⁰C. The decomposition of GO starts at TG onset 161⁰C with the weight loss 14.6 %.The first step decomposition occurs in the temperature range of 161⁰C -233⁰C. 14.6 % weight loss was found in this temperature range. Within this range of temperature, the oxygen bearing functionalities presenting over the graphitic surface of GO has been removed, converting this into graphite. On further heating of GO from 233 °C to 441 °C with weight loss of 10.9 %, a steep loss has been recorded, due to the oxygen containing groups. CO_2 (2350 cm^{-1} and 690 cm^{-1}) and H_2O (1340-1900 cm^{-1} and 3550-4000 cm^{-1}) are the products of this decomposition as expected in the FTIR spectra of GO (Figure 4.2.3). Beyond this temperature, the thermal degradation of GO was proposed with rapid weight loss 49 % till TG endset 566⁰C for the second step decomposition. The decomposition of GO was at 1000 °C leaving the residue 13.74 due to formation of carbon black.

GOMNCs (I) starts decomposition at TG onset of 100⁰ C with the weight loss 3.8 % (Fig. 4 (a)). It may be due to the presence of water molecules in the nanocomposites. Afterwards, the 6.2 % weight loss occurs in the temperature range of 100⁰C-359⁰C. Beyond this temperature, it occurs in the temperature range of 100⁰C-359⁰C. Beyond this temperature, it is decomposed with a rapid weight loss of 7.7% till TG endset temperature 472⁰ C. On further heating, there is no weight loss. For GOMNCs (III), only 3.02 % weight loss was observed up to 100⁰ C (Fig. 4 (a)). Beyond this temperature, 4.24 % weight loss occurs till the 300⁰ C. On further heating, it was degraded with the weight loss 6.74% till the endset temperature 471⁰C. Thus, a remarkable

increase in thermal stability of GOMNCs (III) was observed over GOMNCs (I). Decomposition of GO was terminated in the temperature range 441-566⁰C leaving char residue of (% , w/w) 14.4, whereas GOMNCs (I) and GOMNCs (III) leaves char residue of 82.5 and 86 at 472⁰C and 471⁰C, respectively.

In order to have the comparative study of thermal stability of the GO based composites , their respective TG data were compared at 300 ⁰C and 600 ⁰C (Fig.4. (a)). At the 300 ⁰C weight residue (%) GO, Magnetite , GOMNCs (I) and GOMNCs (III) are 68, 97.8, 91. and 92.74. This remarks the higher thermal stability of magnetite over GO and overall thermal stability of the GOMNCs. At 600⁰ C weight losses (%) associated with GO, Magnetite , GOMNCs (I) and GOMNCs (III) 85, 2.04, 17.5 and 14.04 respectively. Such weight losses associated higher thermal stability of GO-Fe₃O₄ (III) over GO-Fe₃O₄ (I). On further heating, no weight loss was observed for GO and GOMNCs. Thus, synthesized nanocomposites display higher stability over GO.

GOMNCs (I) revealed the heat of decomposition of -1.17 J/mg at 417⁰ C with the DTA signal 4.8 μ V respectively (Fig. 4. (b), (c)). GOMNCs (III) shows two DTA peaks at 428 ⁰C and 516 ⁰C with 42.2 μ V and 10.7 μ V accompanied by heat of composition -922 mJ/mg and -44.5 mJ/mg respectively. Such increase in heat of decomposition DTA peak temperature also further accounted for the increase in the thermal stability of the graphene based nano composites with the proportional to magnetite nanoparticles. DTG revealed the rate of decomposition (μ g/min) for GOMNCs (I) is 67 and 110 corresponding peak temperatures (⁰C) 63 and 429.

Magnetic properties : Fig.5 shows the magnetic field dependence of magnetization (M-H) curves of MNPs and GOMNCs. The magnetization was recorded at 300K with the maximum field of 40K Oe. The samples exhibit immeasurable values of coercive field and remnant magnetization which shows the superparamagnetic nature of all samples [50]. The saturation magnetization of the GOMNCs (I) and GOMNCs (III) [\sim 38 emu/g and \sim 46 emu/g respectively] is smaller than the value of bulk MNPs [\sim 70.5 emu/g] [44]. It is observed that saturation magnetization value in GOMNCs decreases by adding GO into the MNPs [51,52]. This can be attributed to the small particle size and relatively low amount of MNPs in the GOMNCs.

Dielectric Properties: Dielectric permittivity (ϵ') and loss tangent ($\tan \delta$) of the GOMNCs as the function of frequency at the room temperature are shown in Fig.6. The dielectric permittivity, which is also known as the relative dielectric constant, is the real part of the complex dielectric permittivity ($\epsilon = \epsilon' - j\epsilon''$). The Loss tangent ($\tan \delta = \epsilon''/\epsilon'$) is commonly used as a measure of the energy dissipation in the dielectric materials. From fig. 6 remarked the dielectric permittivity for GOMNCs get enhanced with the MNPs. It could also be noted that the dielectric loss (Fig. 6 (b)) of these composite system shows the little improvements with the addition of MNPs. This may be due to the rotation of Fe^{3+} - Fe^{2+} dipoles. It may be viewed as the interchange of electrons between the ions so that the dipoles align themselves with the field. Thus the higher value of dielectric constant at low frequency is mainly due to the space charge polarization and rotation direction polarization. The contribution of rotation direction polarization becomes less at higher frequency because the dipole now cannot follow the quickly changing electric field so we obtained a decreasing pattern of ϵ' with increasing frequency. The dielectric loss is found to be decreased with the addition of MNPs into the composite system. This reveals that the high dielectric loss observed in the GOMNCs. It may also be due to the electronic conductivity of GO. With the addition of MNPs leads the reduction of electronic conductivity of the composites. The variation of ϵ' and dielectric loss with frequency is similar to the behavior of graphene-oxide/ $\text{Zn}_x\text{Fe}_{1-x}\text{Fe}_2\text{O}_4$. It can be evident from this study that dielectric properties can be tuned according to MNPs.

Conclusion: This study is investigated the synthesis of super paramagnetic graphene oxide with magnetite nanoparticles prepared by the co-precipitation method. Surface morphology, X-ray diffraction and fourier transform infrared spectra displayed the magnetite nanoparticles are successfully attached with the graphene oxide. Synthesized nano system the different magnetic and dielectric properties with their pristine form. The graphene oxide based magnetite nano composites with superparamagnetic behavior provide the opportunities for various applications in the fields of biomedicine, drug delivery, tumor treatment, bio-material separation and bio-diagnostics, etc.

References:

1. S. Tanwar, D. Mathur *Mat. Today: Proc.*, **30(1)**, 2020, Pages 17-22.

2. G. Bisht, M.G.H. Zaidi, S. Rayamajhi. *Int. J of Polymeric Mat. and Polymeric Biomat.*, 66 (14): 708 (2017).
3. B. Vestince, Mbayachi, E. Ndayiragije, T. Sammani, S. Taj, E. R. Mbuta, A. U. Khan. *Results in Chemistry*. 3, 2021, 100163.
4. A. R. Urade, I. Lahiri, K. S. Suresh. *Springer Nature*. 2022 14;75(3):614–630.
5. V. Rani, I. Joshi, P. S. Rawat, R. C. Srivastava. *Bulgarian Chemical communications* 55(A):2023.
6. S. K. Joshi, A. Kumar, M.G.H. Zaidi. *Defense Sci. J.*, **70**(3), 306 (2020).
7. H. Mudila, P. Parashr, H.L. Kapoor, S. Rana, M.G.H. Zaidi. *Port. Electrochem. Acta*, **38**(2), 69 (2020).
8. I. Joshi, V. Rani, P. Joshi, K. Khatri. *Bulgarian Chemical Communications* 55(A):2023.
9. M. Mahdavi, M. B. Ahmad, M. J. Haron, F. Namvar, B. Nadi, M. Zaki, A. Rahman, and J. Amin. *Molecules* 2013, 18(7), 7533-7548.
10. L. León Félix, B. Sanz, V. Sebastián, T. E. Torres, M. H. Sousa, J. A. H. Coaquira, M. R. Ibarra, G. F. Goya. *Scientific Reports.*, **9**, 4185 (2019)
11. K. A. Abro, I. Khan, J. F. Gomez-Aguilar. *J. Ther. Ana. and Cal.*, **143**(5), 3633 (2021).
12. P. Kulal, V. Badalamoole. *Int. J. Bio. Macromolecules.*, **165**, 542 (2020).
13. N. Ahmadpour, M. H. Sayadi, S. Sobhani, M. Hajiani. *J. Env. Management.*, **271**, 110964 (2020).
14. G. Bisht, M.G.H. Zaidi. *Drug Delivery and Translational Res.*, **5**, 268 (2015).
15. A.C.S. Costa, H.P.A. Alves, M. A. Correa, F. Bohn, W. Acchar. *Mat. Chem. and Phy.*, **232**, 1 (2019).
16. V. Chandra, J. Park, Y. Chun, J.W. Lee, I.-C. Hwang, K.S. Kim. *ACS Nano.*, **4**, 3979 (2010).
17. Y. Yunjin, M. Shiding, L. Shizhen, M. Li Ping, S. Hongqi, W. Shaobin. *Chem. Engi. J.*, **184**, 326 (2012).
18. N.I. Zaabaa, K.L. Foa, U. Hashima, S.J. Tan, Wei-Wen Liua, C.H. Voona. *Procedia Engineering*, 184 (2017) 469 – 477
19. Syed Nasimul Alam, Nidhi Sharma, Lailesh Kumar. *Graphene*. 6 (1) 2017

20. Rahman, O. U., Mohapatra, S. C. and Ahmad S. 2012. *Materials Chemistry and Physics*.132:196– 202.
21. Shahid, A., Iftikhar, H. G., Nasir, M. and Muhammad, M. 2015. *Materials Characterization* .99: 254–265
22. C. H. Manoratne , S.R.D.Rosa and I.R.M. Kottegoda *Material Science Research India* Vol. 14(1), 19-30 (2017)
23. V. Rani, R. C. Srivastava, H. M. Agarwal, M.G.H. Zaidi. *Mat. Today: Proc.*, **4** (9), 9471 (2017).
24. V. Rani, I. Joshi, P.S. Rawat, R. C. Srivastava . *Bulgarian Chemical communications* 55(A):2023

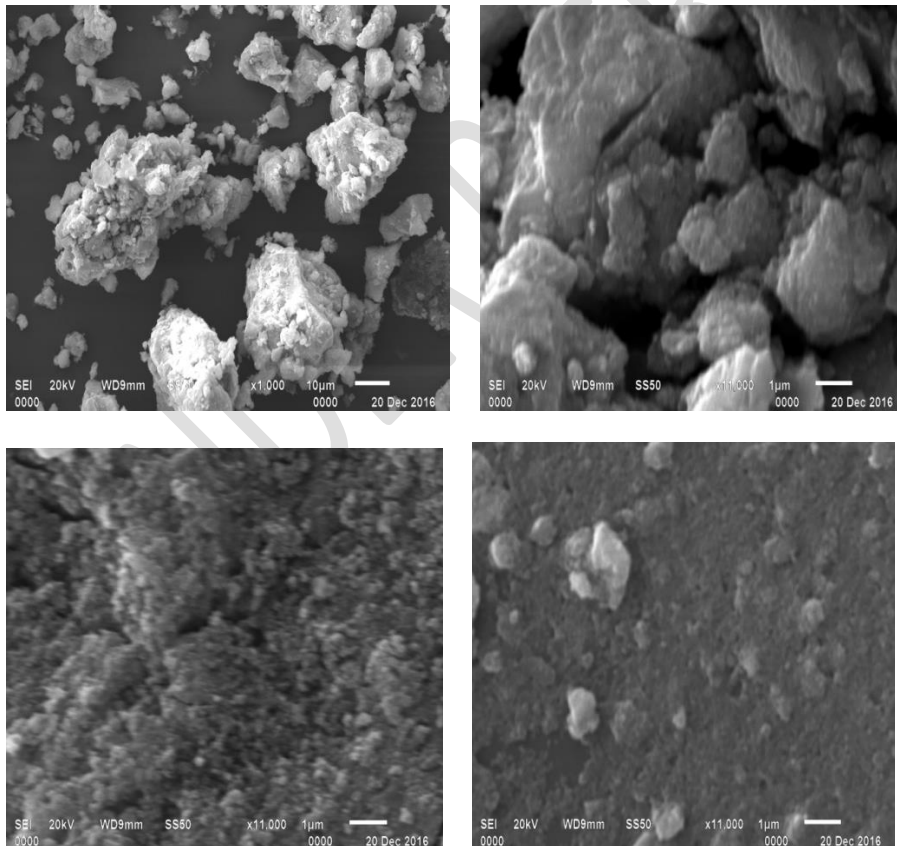


Figure 1 SEM images of GO-Fe₃O₄ nano-composites at different magnifications

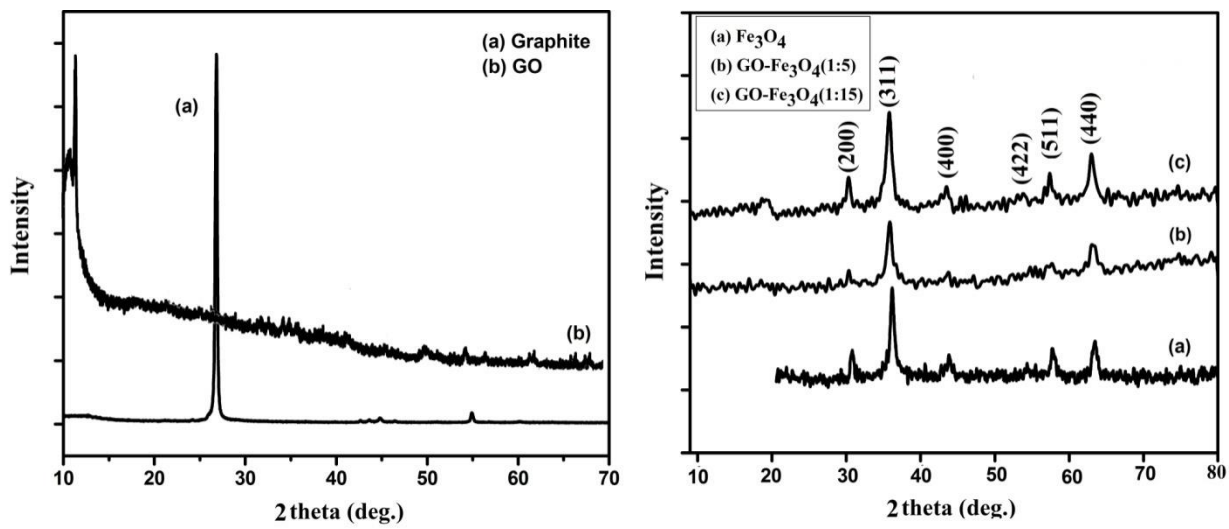


Figure 2: XRD of Graphite, Graphene Oxide and GO-Fe₃O₄ nanocomposites

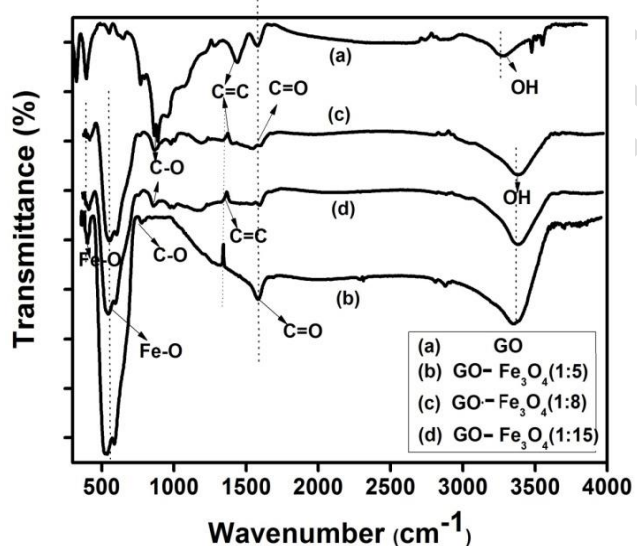


Figure 3: FTIR Spectra of GO and GO-Fe₃O₄ nanocomposites

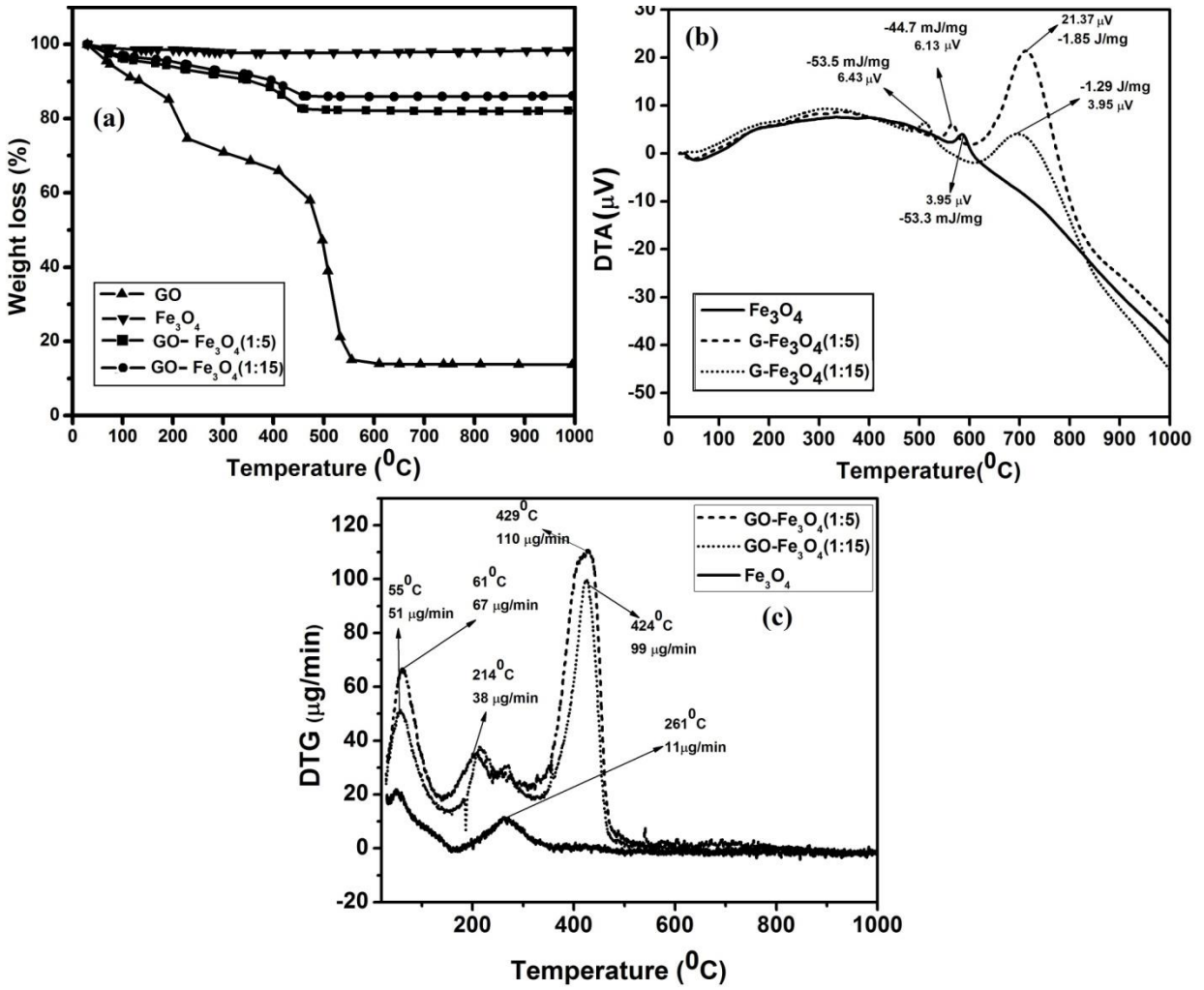


Figure 4: TGA, DTA and DTG graph of GO and GO- Fe_3O_4 nanocomposites

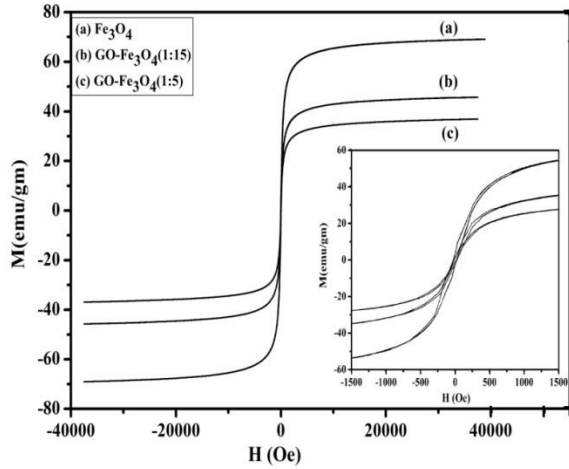
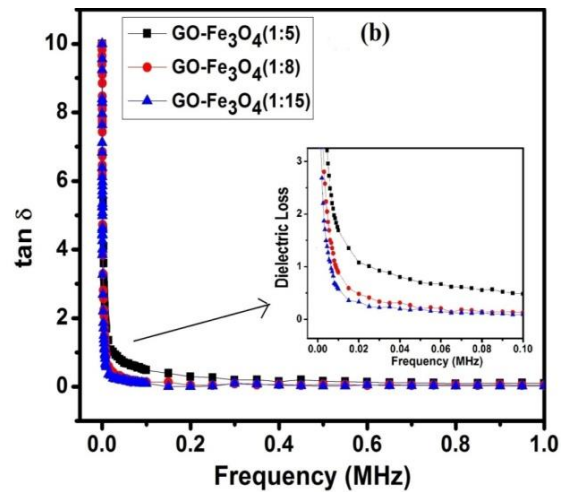
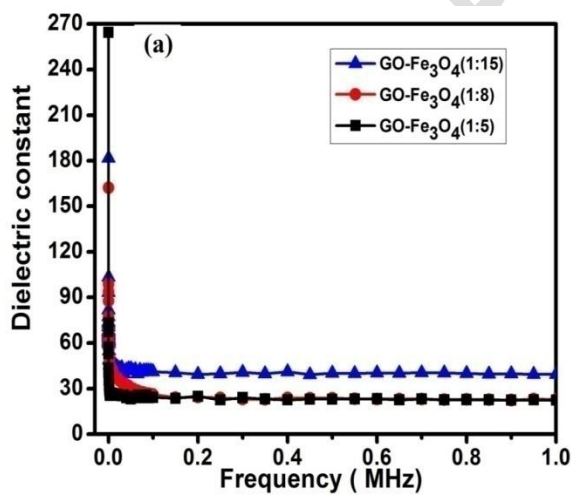


Figure 5: VSM of Fe₃O₄ and GO-Fe₃O₄ nanocomposites .

Samples	Saturation Magnetization (emu/gm)	Standard error	Coercivity (Oe)	Remnant Magnetization (emu/gm)	M _r /M _s
Fe ₃ O ₄ NPs	70.403	0.158	25.384	3.469	0.0493
GOMNCs (I)	37.868	0.057	14.051	1.294	0.0342
GOMNCs (III)	46.560	0.083	19.042	1.748	0.0375

Table 1- Magnetic properties of Fe₃O₄ NPs and GOMNCs (I) and GOMNCs (III)



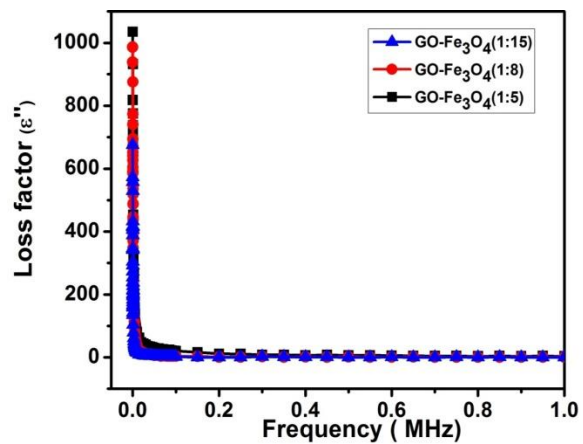


Figure 6: Dielectric Constant and (b) Dielectric loss variation with Frequency (307 K) for GO-Fe₃O₄ nanocomposites.